

Temporal Changes in Gene Expression after Injury in the Rat Retina

Félix Vázquez-Chona, Bong K. Song, and Eldon E. Geisert, Jr

PURPOSE. The goal of this study was to define the temporal changes in gene expression after retinal injury and to relate these changes to the inflammatory and reactive response. A specific emphasis was placed on the tetraspanin family of proteins and their relationship with markers of reactive gliosis.

METHODS. Retinal tears were induced in adult rats by scraping the retina with a needle. After different survival times (4 hours, and 1, 3, 7, and 30 days), the retinas were removed, and mRNA was isolated, prepared, and hybridized to the Affymatrix RG-U34A microarray (Santa Clara, CA). Microarray results were confirmed by using RT-PCR and correlation to protein levels was determined.

RESULTS. Of the 8750 genes analyzed, approximately 393 (4.5%) were differentially expressed. Clustering analysis revealed three major profiles: (1) The early response was characterized by the upregulation of transcription factors; (2) the delayed response included a high percentage of genes related to cell cycle and cell death; and (3) the late, sustained profile clustered a significant number of genes involved in retinal gliosis. The late, sustained cluster also contained the upregulated crystallin genes. The tetraspanins *Cd9*, *Cd81*, and *Cd82* were also associated with the late, sustained response.

CONCLUSIONS. The use of microarray technology enables definition of complex genetic changes underlying distinct phases of the cellular response to retinal injury. The early response clusters genes associate with the transcriptional regulation of the wound-healing process and cell death. Most of the genes in the late, sustained response appear to be associated with reactive gliosis. (*Invest Ophthalmol Vis Sci.* 2004;45:2737-2746) DOI:10.1167/iovs.03-1047

In response to local injury, the retina presents a characteristic series of changes at the site of injury. A secondary series of changes then spreads to involve the entire retina, often resulting in progressive degenerative changes and the formation of scar tissue.¹⁻⁶ These responses of the retina to injury can be divided into an early acute phase, a delayed subacute phase, and a late chronic phase.^{1,4,6}

The early phase, which occurs within the first few hours after injury, is characterized by hemorrhage,^{1,3,5} alterations in the glutamatergic system,⁷ changes in ionic balance,⁸ and the beginning of cell-death cascades.^{9,10} It is during this early

phase that the first changes in the transcriptome occur, with upregulation of the immediate early genes.^{9,10} The retina then undergoes a series of delayed cellular responses that last for days. Among these responses is a generalized inflammatory reaction in which damaged cells release proinflammatory cytokines that recruit peripheral blood components.^{1,3,6} Many retinal cells experience cell-type-specific responses: dedifferentiation, degeneration, migration, hypertrophy, and proliferation.^{4,9,11-13} For example, Müller glial cells and the retinal pigmented epithelium (RPE) enter a reactive state in which they change protein expression, proliferate, and migrate into the wound and vitreous space.^{4,6,11,12} Inflammation and cell proliferation resolve within the first week as the response to injury enters its chronic phase.^{1,4,6} During the late phase, RPE and Müller cells remain reactive and participate in structural remodeling of the retina. Cells that migrate into the wound and vitreous space replace the hemorrhage with fibrocellular membranes.^{1,4,6,12} With time, these membranes may contract, causing significant problems, including retinal detachment.^{1,4,6,12}

Progress in understanding the mechanisms controlling secondary injury has been significant. Gains have come about by focusing on individual molecules^{5,14-16} or groups of molecules^{7-9,17} and their participation in specific processes of the retinal healing response. However, many of the molecular events associated with activation of this response remain unknown. In the present study, we used microarray technology to catalog the expression of thousands of genes after retinal injury. Our first approach was discovery-driven, using the power of microarray to define the global patterns of gene expression changes. The second approach was hypothesis-driven, focusing on the role of *Cd81* (whose product is involved in proliferation and gliosis^{15,16,18-20}) and markers of reactive gliosis, including the cytoskeletal protein glial fibrillary acidic protein (GFAP).^{1,5,11,14,21,22}

METHODS

Animals and Surgery

We used 59 male Sprague-Dawley (albino) rats (270–330 g) and 2 Long-Evans (pigmented) rats (350–400 g)—the latter in examining the response of the RPE to retinal injury (Table 1). We anesthetized 47 albino rats and 2 pigmented rats by intraperitoneal injection of a mixture of xylazine (13 mg/kg) and ketamine (87 mg/kg), then induced a retinal tear in both eyes of each rat. For this purpose, we used a 27-gauge needle to penetrate the pars plana, then scraped the superior temporal retina medially to laterally, as previously described.^{15,16,21,22} Care was taken to prevent lens and sclera damage. Twelve control animals received no injury. All animals were killed by intraperitoneal injection of a mixture of xylazine (26 mg/kg) and ketamine (174 mg/kg). All protocols used in this study were approved by the Animal Care and Use Committee of the University of Tennessee Health Science Center and were in accordance with the ARVO Statement for the Use of Animals in Ophthalmic and Vision Research.

Microarray Expression Profiles

Arrays, Sample Preparation, and Hybridization. Using the rat RG-U34A oligonucleotide array (Affymetrix, Santa Clara, CA),

From the Department of Ophthalmology, University of Tennessee Health Science Center, Memphis, Tennessee.

Supported by National Eye Institute Grant R01EY12369 (EEG), Core Grant 5P30 E7013080-04S1, and by an unrestricted grant from Research to Prevent Blindness, Inc.

Submitted for publication September 23, 2003; revised February 4, 2004; accepted March 9, 2004.

Disclosure: F. Vázquez-Chona, None; B.K. Song, None; E.E. Geisert, Jr, None

The publication costs of this article were defrayed in part by page charge payment. This article must therefore be marked "advertisement" in accordance with 18 U.S.C. §1734 solely to indicate this fact.

Corresponding author: Eldon E. Geisert, Jr, Department of Ophthalmology, University of Tennessee Health Science Center, 855 Monroe Avenue, Memphis, TN 38163; egeisert@utmem.edu.

TABLE 1. Experiments and Distribution of Animals

Experiment	Animals	Survival Time
Gene expression	Albino: 30 injured,* 6 control*	4 Hours, and 1, 3, 7, and 30 days
Protein expression	Albino: 6 injured,† 6 control†	7 Days
Histology	Albino: 8 injured,‡ 3 control	1, 3, 7, and 30 days
RPE response	Pigmented: 2 injured	7 Days

* Six animals per experimental condition. For each experimental condition, we processed three independent retinal samples with two animals per sample.

† For each experimental condition, we processed three independent retinal samples with two animals per sample.

‡ Two animals per experimental condition.

we examined gene expression levels in the normal rat retina and injured rat retinas with 4-hour and 1-, 3-, 7-, and 30-day survival time (Table 1). Retinas used for expression studies were dissected and examined under a stereomicroscope (model SXZ12; Olympus, Tokyo, Japan) and immediately processed. Nissl-stained sections of the eye-cups showed that our retinal dissections included both the neural retina and RPE. We collected retinas from 36 animals—6 animals per experimental condition. For each experimental condition, we processed three independent retinal samples with two animals per sample. Thus, we collected 18 biological replicates and performed 18 hybridizations (Supplemental Table 1 at www.iovs.org/cgi/content/full/45/8/2737/DC1). We performed total RNA extraction (TRIzol; Invitrogen, Carlsbad, CA) and confirmed the integrity of RNA with a bioanalyzer (model 2100; Agilent Technologies, Palo Alto, CA). We synthesized, labeled, and hybridized cRNA onto arrays at Genome Explorations (Memphis, TN) according to standard Affymetrix methods, previously described by Rogojina et al.²³

Data Extraction and Normalization. We measured gene expression levels on computer (Microarray Suite 5.0; MAS 5.0; Affymetrix) and robust multiarray average (RMA)²⁴ algorithms. Signals were log transformed (base 2), and the mean intensity for each microarray was normalized to 8 (log₂ scale).²³

Statistical and Clustering Analyses. We determined the statistical significance of expression changes using Student's *t*-test statistics. To determine the expected proportion of significant false positives, we used the false-discovery rate of Benjamini and Hochberg.²⁵ Significantly expressed genes were clustered with CLUSFAVOR 6.0,²⁶ using principal component analysis (PCA). Averages are expressed mean ± SEM.

MIAME Compliance and Availability of Microarray Data.

For further discussion on experimental design and other details of methods (MIAME report), see the online Appendix at www.iovs.org/cgi/content/full/45/8/2737/DC1. The raw MAS 5.0 data set is publicly available at Gene Expression Omnibus (www.ncbi.nlm.nih.gov/geo/) provided by the National Institute of Health, Bethesda, MD) as the group series GSE1001 (for individual accession numbers, see Supplemental Table 1).

One-Step RT-PCR

Using fluorescent, one-step reverse transcription-polymerase chain reaction (RT-PCR), we verified microarray expression changes for the early-response genes *Fos* and *Fos11*, delayed-response genes *Il1b* and *Irf1*, and late-sustained response genes *Cryab*, *Crygd*, *Cd81*, and *Gfap* (nucleotide sequences shown in Supplemental Table 2 at www.iovs.org/cgi/content/full/45/8/2737/DC1). We performed primer design, one-step RT-PCR reaction, and RT-PCR analysis as previously described by Rogojina et al.²³ To eliminate genomic contamination, we treated total RNA with RQ1 RNase-free DNase (Promega, Madison, WI). We performed RT-PCR reactions in a thermocycler (iCycler; Bio-Rad, Richmond, CA), using the reagents in the SYBR Green RT-PCR kit; Applied BioSystems, Warrington, UK). To determine the relative change in gene expression, we used the system software to compare the number of cycles (C_t) needed to reach the midpoint of the linear phase. All observations were normalized to the housekeeping gene *Rps18*.

Protein Expression and Localization

To determine the levels of protein expression in normal retinas and those at 7 days after injury, we used rabbit polyclonal antibody against glial fibrillary acidic protein (GFAP; Thermo Shandon, Pittsburgh, PA), a mouse monoclonal antibody AMP1 that recognizes CD81,¹⁹ and rabbit polyclonal antibodies against crystallin- α , - β , and - γ (provided by Sam Zigler, National Institutes of Health). The secondary antibodies were peroxidase conjugated goat anti-rabbit IgG, and goat anti-mouse IgG (Jackson ImmunoResearch Laboratories, Inc., West Grove, PA), all of which had minimal cross-reactivity with rat serum proteins. We compared protein expression in injured retinas to control retinas using a previously described immunoblot method.^{15,16,19}

Indirect immunohistochemical methods were used to define the cellular localization of GFAP and crystallins in sections of normal and injured retinas. Injured rats had survival times of 1, 3, 7, and 30 days after retinal injury (Table 1). We anesthetized eight injured rats and three control rats, processed tissue, and followed immunohistochemical methods, as previously described.^{15,16,19} For fluorescence microscopy, we used fluorescein-conjugated donkey anti-rabbit IgG (Jackson ImmunoResearch Laboratories, Inc.). To identify RPE cells, we used a rhodamine-conjugated lectin from *Phaseolus vulgaris* (PHA-E; Sigma-Aldrich, St. Louis, MO), and mouse monoclonal anti-cytokeratin antibodies (CBL 234 and MAB 3412; Chemicon, Temecula, CA). We labeled nuclei with a fluorescent Nissl counterstain, Hoechst 33342 (Sigma-Aldrich), and examined the sections with a confocal laser scanning microscope (MRC-1024; Bio-Rad).

RESULTS

Glial and RPE Response to Retinal Injury

To characterize the local and global response to retinal injury, we examined the distribution of retinal glia and RPE cell markers. In normal retinas, anti-GFAP labeled astrocytes and Müller cell end feet in the ganglion cell layer (GCL; Fig. 1A). PHA-E lectin stained the normal RPE, choroid, and outer segments (Fig. 1B, OS)—a pattern similarly described by Cho et al.²⁷ After injury, the local response involved glia and RPE cells. As early as 3 days after injury, cells invading the retinal tear were labeled with anti-GFAP (Fig. 1D, arrow) or PHA-E lectin (Fig. 1E, arrow). Levels of GFAP and PHA-E labeling continued to increase so that by 30 days after injury, two cellular responses were observed at the site of injury. In one response, the cells filling the tear (Fig. 1I, arrowheads) were mainly GFAP-positive glia cells (Fig. 1H, arrowheads). In the second response, RPE cells mainly filled the tear (Fig. 1K, 1L, arrows) and glia cells formed a well-defined membrane separating the scar from the neural retina (Fig. 1J). RPE cell response after retinal injury was consistent with the distribution of pigmented cells in injured Long-Evans rats (data not shown). In some instances, epiretinal membranes with glia (Fig. 1G, arrow) and RPE cells (Fig. 1H, arrow) formed projecting into the vitreous. Thus, local re-

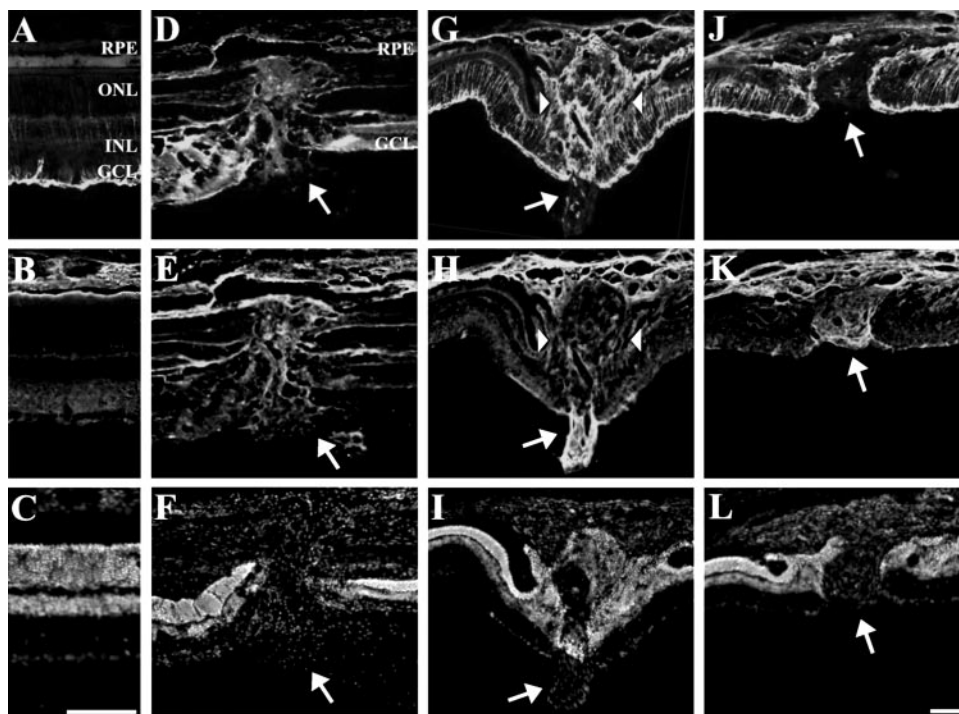


FIGURE 1. The responses of the rat retina to injury. Retinas labeled with anti-glia fibrillary acidic protein (GFAP; A, D, G, J), lectin from *Phaseolus vulgaris* (PHA-E; B, E, H, K), and Hoechst nuclear staining (C, F, I, L). Shown are four regions of retina: normal (A–C), 3 days after injury (D–F), and two different retinas 30 days after injury (G–I, J–L). In normal retinas, anti-GFAP labeled astrocytes and Müller cell end feet at the GCL (A). PHA-E lectin stained the normal RPE, choroid, and outer segments (OS, B). At 3 days after injury, cells invading the retinal tear (F, arrow) labeled with anti-GFAP (D, arrow) or PHA-E lectin (E, arrow); whereas, near the injury anti-GFAP labeled mainly Müller cells and astrocytes at the GCL (D). At 30 days after injury, two cellular responses were observed at the site of injury. In one response, the cells filling the tear (I, arrows) were mainly glia cells (H, arrowbeads). In the second response, RPE cells mainly filled the tear (K and L, arrows). In some instances, epiretinal membranes with glia (G, arrow) and RPE cells (H, arrow) formed over the retinal surface. A–C are of the same magnification and (D–L) are of the same magnification. Scale bar: (A, L) 50 μ m.

sponse to retinal injury involved glia and RPE cells in a manner consistent with previous studies.^{16,28}

In addition to the local response, we observed the spread of GFAP immunoreactivity throughout the retina. During the first 3 days after injury, GFAP labeling was limited to Müller cells adjacent to the injury and to astrocytes in the GCL (Fig. 1D, arrow). At 7 and 30 days after injury, we observed a global GFAP labeling of the retina localized to astrocytes in the GCL, and to Müller cell processes (Fig. 1G, 1J). Near the site of injury, GFAP labeling showed that the Müller cell processes became thicker and extended into the subretinal space, whereas GFAP labeling of peripheral Müller cells extended from the GCL to the photoreceptor layer.

Microarray Expression Profiles

In our analysis of microarray data, we used two different tactics: a discovery-driven approach and a hypothesis-driven approach. In the discovery-driven approach, we defined different patterns of gene expression across the data set, clustering genes that might be functionally related. The hypothesis-driven approach focused on the gene expression of *Cd81* and its relationship with reactive gliosis markers, particularly *Gfap*. This approach allowed us to concentrate on one aspect of the injury response to define the relationships within the tetraspanin family and markers of the reactive glial response.

Quality Controls. The expression profiles ($n = 18$ arrays) met a strict set of quality-control parameters (Table 2). House-keeping genes displayed consistent values and 5' to 3' ratios of

less than 3. The average percentage of Affymetrix-present calls across all arrays was $40.0\% \pm 1.1\%$. The intensity profiles (\log_2 scale) for all the arrays showed a normal distribution, with a mean at 6.59 ± 0.04 and an average SD (σ^2) of 2.32 ± 0.04 . Comparison of expression profiles among arrays from independent replicates of the same experimental group ($n = 3$ arrays/group) showed a within-group average correlation of 0.92 ± 0.01 . Our quality controls are consistent with published microarray data.^{10,29,30} Together, these results indicate integrity of starting RNA, and efficiency of first-strand cDNA synthesis and hybridization.

Data Extraction and Normalization. For temporal analysis of the data and comparison between data extraction methods, the mean intensity for each microarray was normalized to 8 (\log_2 scale). This transformation yielded MAS 5.0 signal intensities ranging from 1 to 18 relative units of fluorescence. To determine a “present” signal threshold in our system, we plotted the coefficient of variation versus the averaged signal value and determined the threshold signal yielding stable coefficients of variation. From this analysis, the present signal threshold was set at 8.64. Below this threshold, signals displayed coefficients of variation greater than 10%, whereas their variance increased exponentially (Supplemental Fig. 1 at www.iovs.org/cgi/content/full/45/8/2737/DC1). Using this criterion, 4480 (50.9%) of the genes met the present criterion in at least one condition and were considered for further analysis. We compared the present expression signals to RMA values and found an average correlation of 0.92 ± 0.01 (Supplemental Table 3 at www.iovs.org/cgi/content/full/45/8/2737/DC1).

TABLE 2. Microarray Expression Profiles in the Retina after an Experimentally-Induced Retinal Tear

Parameters	Survival Time						
	Control	4 Hours	1 Day	3 Days	7 Days	30 Days	Combined
Average group quality controls							
<i>Actb</i> 3'/5' signal ratio	1.84 ± 0.09	1.90 ± 0.09	2.08 ± 0.07	2.43 ± 0.44	2.03 ± 0.05	2.14 ± 0.05	2.07 ± 0.08
<i>Gapdh</i> 3'/5' signal ratio	1.11 ± 0.24	0.84 ± 0.02	0.86 ± 0.02	1.21 ± 0.15	1.03 ± 0.12	1.05 ± 0.01	1.02 ± 0.05
Array signal mean	6.62 ± 0.09	6.65 ± 0.05	6.55 ± 0.07	6.59 ± 0.04	6.66 ± 0.20	6.50 ± 0.03	6.59 ± 0.04
Array signal distribution (σ^2)	2.30 ± 0.08	2.30 ± 0.03	2.38 ± 0.05	2.33 ± 0.02	2.21 ± 0.21	2.41 ± 0.01	2.32 ± 0.04
Affymetrix % present	37.0 ± 1.8	37.9 ± 1.4	43.2 ± 1.2	42.2 ± 3.6	38.2 ± 5.5	41.8 ± 0.3	40.0 ± 1.1
Correlations	0.89 ± 0.02	0.94 ± 0.01	0.95 ± 0.00	0.92 ± 0.01	0.89 ± 0.02	0.94 ± 0.00	0.92 ± 0.01
Differentially expressed genes							
“Present” in at least one condition; α -fold change > ±1.71; and <i>t</i> -test, $P < 0.02$		113	127	125	40*	127	393
False-discovery rate (FDR, %)		17.5	16.5	18.0	39.0*	14.0	21.0 ± 5.1

Three biological replicates were used per group. Averages are expressed as the mean ± SEM. MAS 5.0 signals were transformed into the log₂ scale. To determine temporal changes in gene expression, mean intensities were normalized to 8 (log₂ scale) and a signal “present” threshold was set at 8.64 (log₂ scale). The false-discovery rate (FDR) of Benjamini and Hochberg²⁵ was used to determine the expected proportion of false positives.

* While array expressions at 7 days after injury displayed lower number of genes with significant expression changes and higher FDR, the three 7-day arrays met the quality controls, and the expression of housekeeping genes (e.g., *Gapdh*, *Actb*, *Ubc*, *Hprt*, *Sdha*, and *Rpl41*) was consistent with expression found in the other experimental conditions. Thus, there were no empirical data (technical nor biological) to exclude any data from the 7-day experiments.

To analyze further the reliability of our present signals, we compared multiples of change obtained with normalized MAS 5.0 and RMA to those obtained with RT-PCR (Table 3). Using RT-PCR, we measured expression changes for *Fos*, *Fosl1* (*Fra-1*), *Il1b*, *Irf1*, *Cryab*, *Crygd*, *Cd81*, and *Gfap* at 4 hours, 3 days, and 30 days after injury. For these genes, changes (α -fold) measured with normalized MAS 5.0, and RMA values were

highly similar ($r = 0.89$). Both MAS 5.0 and RMA changes were similar in magnitude and direction to the changes obtained with RT-PCR. However, RT-PCR changes had higher correlations with normalized MAS 5.0 ($r = 0.76$) than with RMA ($r = 0.58$). Together, the high correlation between normalized MAS 5.0 values and RMA values and the similarity between microarray multiples of change and RT-PCR changes confirm the reliability of our present signals, which eliminate genes with low expression signals. Thus, we used the normalized MAS 5.0 data for our subsequent analysis.

TABLE 3. Change Comparison among RT-PCR, MAS 5.0, and RMA

Gene	Time Point	Log ₂ Change (α -fold)		
		RT-PCR	MAS 5.0	RMA
<i>Fos</i>	4 h	1.9†	2.1†	1.2†
	3 d	0.3	0.1	(0.2)
	30 d	0.1	0.2	0.0
<i>Fosl1</i>	4 h	6.5†	5.4†	2.3†
	3 d	2.7†	0.5	0.5
	30 d	1.3†	(0.3)	(0.2)
<i>Il1b</i>	4 h	2.1†	2.0†	1.4*
	3 d	2.0*	1.2*	1.2*
	30 d	0.5	0.1	0.7
<i>Irf1b</i>	4 h	1.0*	1.9*	1.0
	3 d	1.2†	2.3*	1.5*
	30 d	0.1*	1.1*	0.2
<i>Cd81</i>	4 h	0.2	0.1	(0.1)
	3 d	1.0*	1.0*	1.2*
	30 d	1.3†	0.9*	0.7*
<i>Cryab</i>	4 h	0.5*	0.8	0.9
	3 d	2.0†	2.7*	2.6*
	30 d	0.5*	2.4*	2.0*
<i>Crygd</i>	4 h	(0.4)*	(0.7)	(0.5)
	3 d	2.7†	2.7†	1.8†
	30 d	1.9*	3.1*	1.5*
<i>Gfap</i>	4 h	1.6†	0.4	0.4
	3 d	2.1†	3.5†	2.8*
	30 d	2.3†	4.1†	3.8†

α -Fold change represents log₂ (injured/normal expression). Data in parentheses represent negative changes (α -fold). Statistical significance compared population means between the control and each survival time (4 h, 3 d, and 30 d).

* Significant change at $P < 0.05$.

† Significant change at $P < 0.01$.

Discovery-Driven Analysis

The overall goal of our discovery-driven approach was to define groups of genes with similar expression patterns. The first step in the analysis defined 393 genes with significant changes in expression levels (change >1.7-fold and $P < 0.02$; Table 2). These differentially-expressed genes represented an average false discovery rate of 21.0% ± 5.1%. Collectively, these genes displayed a range of dynamic expression changes across survival time. The second step involved clustering the 393 genes into groups according to the similarity of their expression profiles. Using principal component analysis, we identified 194 upregulated genes having transcription changes that conformed to one of three major profiles: an early response (Fig. 2A), a delayed response (Fig. 2B), and a late, sustained response (Fig. 2C). Early-response genes displayed a transient surge in expression after the retinal tear, whereas delayed response genes showed moderate upregulation at 4 hours and a delayed transient peak at either 1 or 3 days after injury. In contrast, late, sustained genes displayed peak upregulation at either 3 or 7 days and sustained overexpression at 30 days after injury. A complete list of upregulated genes organized by clusters is found in Supplemental Table 4 at www.iovs.org/cgi/content/full/45/8/2737/DC1.

The distribution of genes by functional category revealed that genes within clusters were functionally related (Fig. 2D). For instance, 75% of the upregulated transcription genes clustered in the early-response profile. Additional functional groups represented in the early response included cell proliferation, apoptosis, and cell-survival mechanisms. Genes highly represented in the delayed-response profile included those regulating cell cycle, cell death, and survival, neural develop-

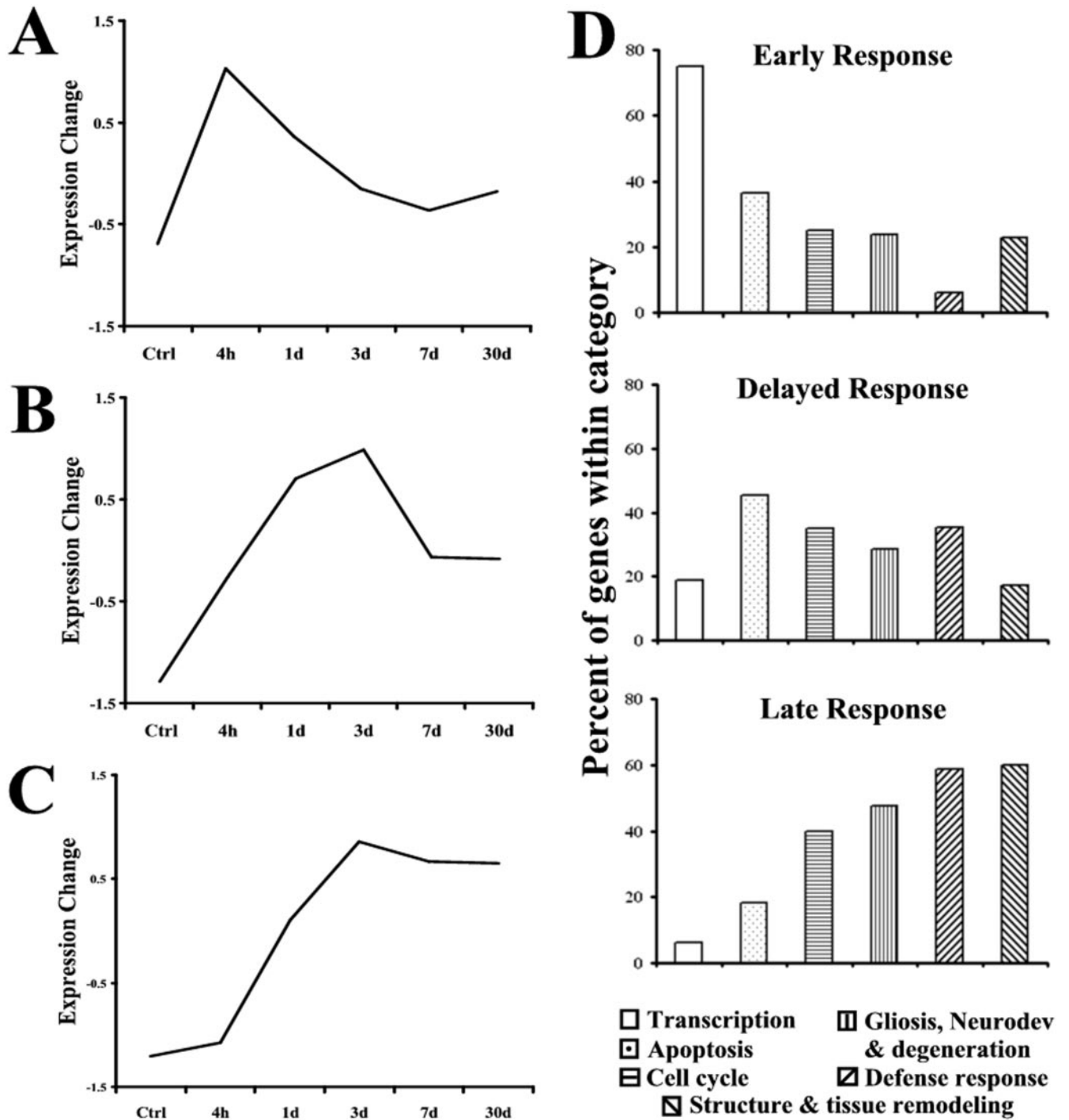


FIGURE 2. Differentially expressed genes ($n = 194$) were clustered into three major profiles: (A) an early response, (B) a delayed response, and (C) a late, sustained response. Genes were clustered using principal component analysis. Early-response genes displayed a transient surge in expression after injury. Genes fitting the delayed-response profile had a transient peak in expression at either 1 or 3 days after injury. Genes within the third expression profile had a late expression peak (i.e., at either 3 or 7 days) and sustained overexpression at 30 days after retinal injury. A complete list of upregulated genes organized by clusters is found online in Supplemental Table 3. The distribution of genes by functional category reveals that those within each expression profile are functionally related (D).

ment, and gliosis. A high percentage of late, sustained genes were associated with the reactive responses of the retina: gliosis, inflammation, stress response, neuronal degeneration, and tissue remodeling. A summary and expanded version of the distribution of genes by clusters and functional category are shown in Figure 3 and Supplemental Table 5 (www.iovs.org/cgi/content/full/45/8/2737/DC1), respectively.

One unexpected finding in our analysis was the clustering of the crystallin genes with the retinal reactive marker *Gfap*. All the crystallins in the microarray—*Cryaa*, *Cryab*, *Cryba1*, *Cryab4*, *Crybb2*, *Crybb3*, *Crygc*, *Crygd*, and *Cryge*—displayed strong, sustained upregulation after the placement of retinal tears (Supplemental Table 5, category 7). To confirm our findings, we examined the mRNA and protein expression of se-

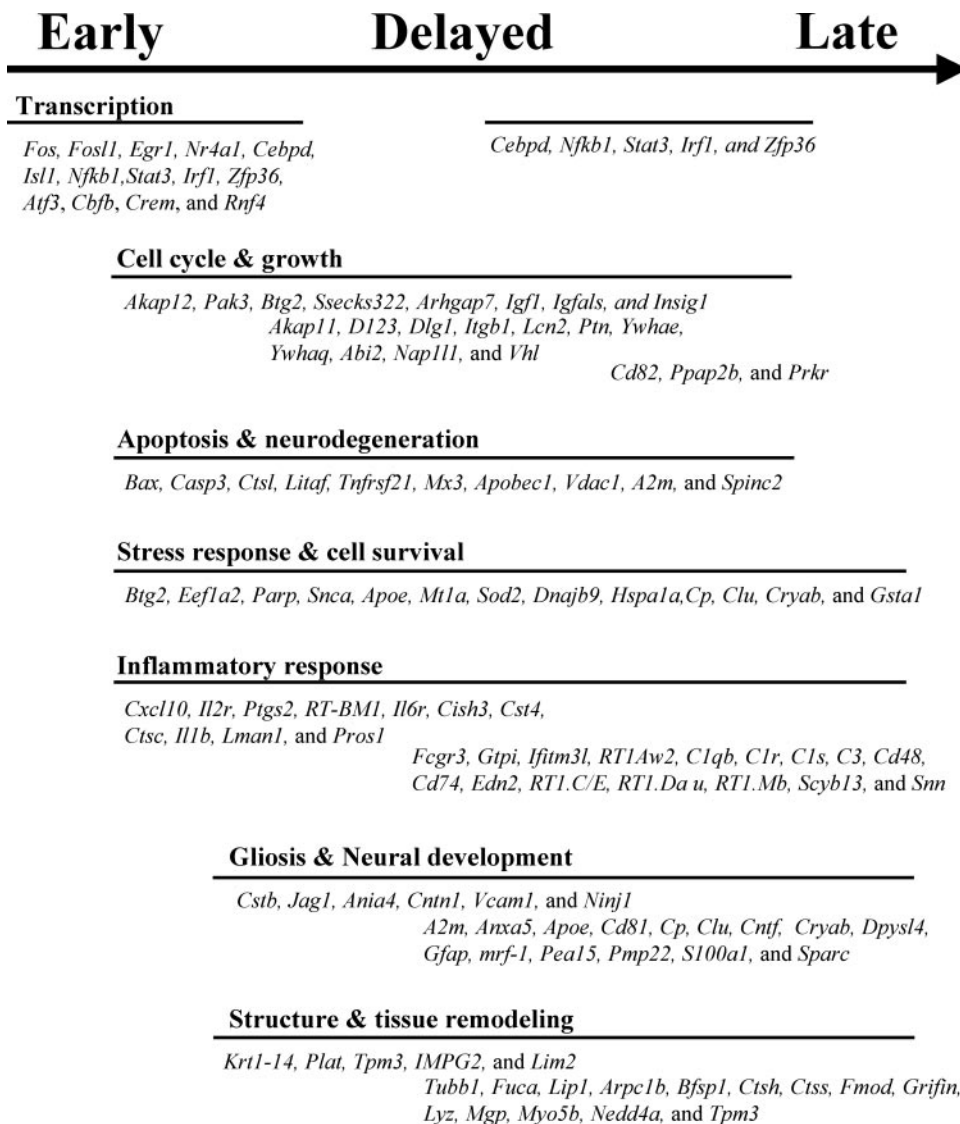


FIGURE 3. Temporal distribution of genes and functional categories after retinal injury. Location of genes describes relative gene expression peaks: early expression corresponds to a peak expression at 4 hours, delayed expression corresponds to a peak expression at 1 or 3 days, and late expression corresponds to a peak expression at 7 or 30 days. For specific expression profiles, see Supplemental Table 4.

lected crystallins. We measured the mRNA expression of *Cryab* and *Crygd*, using RT-PCR. *Cryab* mRNA levels showed a moderate increase of 1.42 ± 0.11 -fold at 4 hours after injury, a robust upregulation of 4.13 ± 0.12 -fold at 3 days, and a moderate change of 1.46 ± 0.04 -fold at 30 days (Fig. 4A). *Crygd* mRNA showed an initial downregulation of 1.34 ± 0.03 -fold, followed by significant changes to 6.36 ± 0.25 -fold at 3 days and 3.64 ± 0.41 -fold at 30 days (Fig. 4A). Our microarray and RT-PCR measurements showed agreement in the direction of change of *Cryab* and *Crygd* (Fig. 4A). Moreover, the mRNA expression of *Cryab* and *Crygd* across time displayed a pattern of expression that was similar to that of genes in our late, sustained profile, with a delayed peak at 3 days and strong, sustained upregulation even after 30 days.

To extend our crystallin gene findings, we measured the protein levels of the crystallin- α , - β , and - γ , using a quantitative immunoblot method (Fig. 4B). The immunoreactivity of each of these crystallins significantly increased to 7.1 ± 0.39 -fold, 6.8 ± 0.66 -fold, and 11.1 ± 2.4 -fold, respectively, at 7 days after injury. Taking this analysis one step further, we defined the localization of the reactivity of crystallin- α , - β , and - γ in normal and injured retinas. In normal retinas, we observed labeling of these crystallins mainly in the GCL (Figs. 4C, 4E, 4G). All three crystallins had well-defined patterns of immuno-

reactivity at the site of injury and within the layers of the retina. At 7 and 30 days after injury, immunoreactivity of these crystallins was seen throughout the scar that spanned the retinal tear and protruded into the vitreous space. Immediately adjacent to the injury, strong crystallin immunostaining was present in the GCL and the photoreceptor layer (Figs. 4D, 4F, 4H; 7-day retinas shown). Moderate levels of immunoreactivity were also observed throughout the inner plexiform layer, the inner nuclear layer, and the RPE. The well-defined pattern of crystallin mRNA upregulation by microarray and RT-PCR as well as the increase of crystallin protein and crystallin localization in the retina by immunohistochemical methods validate our discovery-driven observations that crystallins displayed strong, sustained transcription in response to injury in the rat retina.

Hypothesis-Driven Approach

The primary interest of our laboratory is the role of CD81 in the healing response of the retina. We specifically examined the relationships between *Cd81*, other tetraspanins, and markers of reactive glia. Our microarray data showed that *Cd81* was moderately upregulated at 4 hours, to 1.05 ± 0.1 -fold, and

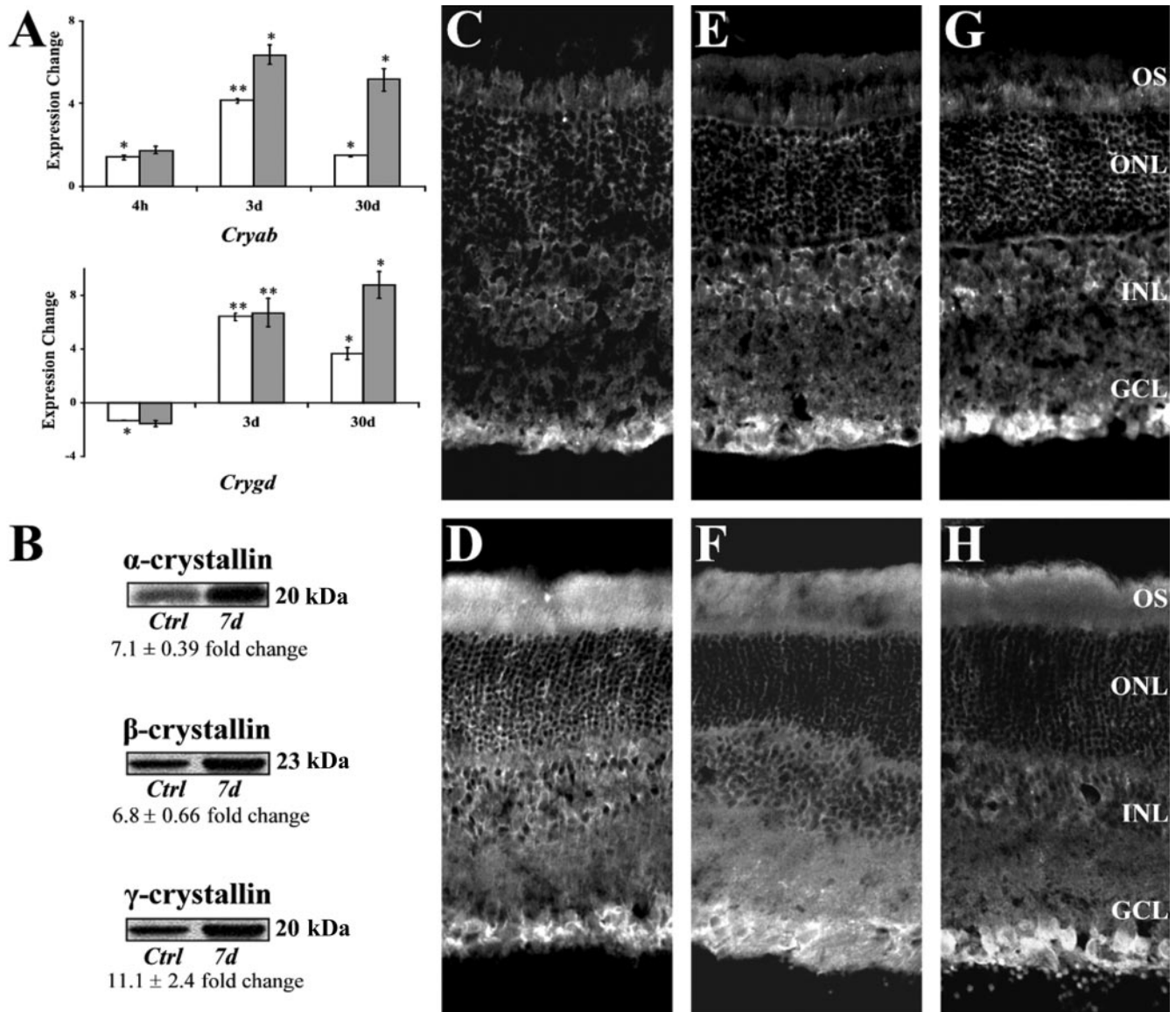


FIGURE 4. Crystallin- α , - β , and - γ were dramatically upregulated after retinal injury. The microarray expression changes for *Cryab* and *Crygd* (A, \blacksquare) were confirmed with RT-PCR (A, \square). Immunoblots show increased levels of crystallin- α , - β , and - γ proteins (B). Crystallin- α , - β , and - γ expression in normal retinas (C, E, G, respectively) and injured retinas 7 days after injury (D, F, H, respectively) was localized by immunohistochemistry. In normal retina, crystallin immunoreactivity was present mainly in the GCL (C, E, G). Seven days after injury, there was a strong crystallin immunoreactivity throughout the scar spanning the retinal tear and protruded into the vitreous space (data not shown). High immunoreactivity levels for crystallin- α (D), - β (F), and - γ (H) were found immediately adjacent to the retina at GCL and outer segment layer (OS). No staining was seen when secondary antibody control was used (data not shown). (A) Significant changes from normal: *t*-test, * $P < 0.05$, ** $P < 0.01$.

significantly increased to 1.99 ± 0.2 -fold and 1.88 ± 0.1 -fold at 3 and 30 days, respectively (Fig. 5A, gray boxes). RT-PCR confirmed the sustained upregulation of *Cd81* mRNA after retinal injury (Fig. 5A, white boxes). Our analysis showed that *Cd81* clustered in the late, sustained profile, along with the tetraspanins and several glial reactive markers (see Supplemental Table 4, genes 126–194). We used a second round of PCA to define further the associations between *Cd81* and the late, sustained profile genes. The subclusters were visualized by plotting the first two components (Fig. 5B). *Cd81* clustered tightly with tetraspanins *Cd9* and *Cd82*, as well as with the genes for associated proteins major histocompatibility complex [MHC] class I (*RT1Aw2* and *RT1.Dau*) and MHC class II (*RT1.C/E*). Together, these genes displayed persistent changes after retinal injury, with peak expression occurring at 3 days

after injury. Tetraspanins *Cd37*, *Cd53*, and *Cd151* were present in the normal retina, but their expression remained constant after injury. Among the glial reactive markers, *Anxa5*, *Cntf*, *Pea15*, *Pmp22*, *S100a1*, and *Sparc* clustered tightly with *Cd81*, whereas *Clu*, *Cryab*, *Gfap*, and *A2m* formed a separate cluster within the late sustained profile (Fig. 5B).

DISCUSSION

The results of our microarray analysis describe both a local reactive response at the site of retinal injury and changes occurring across the entire retina. As with injuries in other parts of the central nervous system (CNS),³¹ a local glial response is identified by the dramatic upregulation of the cy-

have been thought to be lens-rich proteins involved in lens development and maintenance. However, recent studies^{10,46-50} suggest that crystallins have broader roles and are expressed beyond lens tissue. Gene-sequence homology studies of crystallins show that members of this family display considerable homology with genes involved in the stress response.^{46,47} For instance, the α -crystallins belong to the small heat-shock protein family and may act as molecular chaperones.^{46,47} In cultured RPE, α B-crystallin upregulation confers resistance to stress-inducible apoptosis.⁴⁸ A recent gene expression study confirmed the increased expression of selected α , β , and γ crystallin transcripts in the rat retina after ischemia-reperfusion injury.¹⁰ Similarly, we found that the mRNA of all 10 crystallins represented in the microarray displayed strong, sustained upregulation after retinal injury. These results are consistent with the increased crystallin protein expression confirmed by Sakaguchi et al.⁴⁹ using mass spectrometry after exposing rat retina to light injury. Furthermore, the temporal and spatial expression of crystallins is similar to that of GFAP, implicating this family of proteins in both the local and global response of the retina to trauma. Notably, studies of gene expression in the brain²⁹ and spinal cord³⁰ using the identical microarray platform (RG-U34A) did not find a similar upregulation in crystallin- α , - β , and - γ in response to trauma. Whereas crystallin expression in normal mouse retina displays animal-to-animal variation,⁵⁰ studies after retinal detachment,¹⁰ light injury,⁴⁹ and our retinal tear consistently report the upregulation of crystallins. The coordinated upregulation of crystallins after injury is a potentially important part of the retinal wound-healing process that merits further investigation. Defining the response of the crystallin family to injury illustrates the power of microarray technologies and the discovery-driven approach.

Microarray technology, combined with gene expression profiling, offers the potential to identify cellular pathways and molecular complexes that are essential to the regulation of retinal responses to trauma and disease.^{9,10} Our laboratory is defining the role of CD81 in reactive gliosis in the retina,^{15,16} brain,²⁰ and spinal cord.¹⁸ CD81 is part of a molecular complex within the plane of the membrane that links adhesive interactions into second-messenger cascades.^{51,52} Using microarray technology, we monitored gene expression changes for *Cd81* and the entire family of tetraspanins (e.g., *Cd9*, *Cd37*, *Cd53*, *Cd63*, *Cd81*, *Cd82*, and *Cd151*).^{51,52} In addition, we specifically mined the data to define changes in molecules known to associate with this family of proteins to determine whether the members of the tetraspanin complex are coregulated. Our analysis indicates that similar patterns of expression are shared by the tetraspanin genes *Cd9*, *Cd81*, and *Cd82*, as well as genes for the MHC receptors *RT1Aw2*, *RT1.Dau*, and *RT1.C/E* (Fig. 3). Tetraspanins CD81, CD9, and CD82 are known to associate with MHC receptors in a number of different cell types, including lymphocytes, endothelial cells, and oocytes.⁵¹⁻⁵³ For instance, CD81 and CD82 interact with MHC class I and II in antigen-presenting cells to modulate signaling through MHC molecules and antigen presentation.⁵³ Defining the temporal expression of the tetraspanins and the molecules to which they complex allows us to focus on the specific role of CD81 in the retina, its potential molecular associations, and its role in the reactive response.

The present study catalogued the time course of expression changes in response to a retinal injury. By surveying the expression patterns of 8750 genes, we defined an early, a delayed, and a late, sustained response to retinal injury and demonstrated that within each profile, genes participate as functional units involved in different aspects of the healing response. Within the late response profile, we identified a host of glial reactive genes as well as crystallins, a previously overlooked family of proteins in the injured retina. In profiling the

expression of tetraspanins, we identified CD9, CD81, and CD82 as potential organizers of molecular complexes regulating proliferation and the glial activation response. Our finding that crystallins and tetraspanins can act in functional units highlights the fact that the function, or therapeutic intervention, of a gene can be regulated at the gene expression level. However, we are limited in our ability to link crystallins or tetraspanins to specific cell populations or specific pathways. Future research using single-cell studies and genetically altered animals will help dissect the molecular pathways and networks regulating gene expression.

Acknowledgments

The authors thank Samuel Zigler at the National Eye Institute for the gift of the rabbit polyclonal antibodies against crystallins; Grace R. Geisert and William E. Orr for technical assistance; and Edward Chaum and David Twombly for valuable comments on the manuscript.

References

- Ryan SJ, Stout JT, Dugel PV. Posterior penetrating ocular trauma. In: Ryan SJ, ed. *Retina*. Vol 3. St. Louis: CV Mosby Co.; 1994:2235-2250.
- Postel EA, Mieler WF. Posterior segment manifestations of blunt trauma. In: Guyer DR, ed. *Retina-Vitreous-Macula*. Vol 1. Philadelphia: WB Saunders Co.; 1999:831-843.
- Gregor Z, Ryan SJ. Combined posterior contusion and penetrating injury in the pig eye. II. Histological features. *Br J Ophthalmol*. 1982;66:799-804.
- Fisher SK, Stone J, Rex TS, Linberg KA, Lewis GP. Experimental retinal detachment: a paradigm for understanding the effects of induced photoreceptor degeneration. *Prog Brain Res*. 2001;131:679-698.
- Humphrey MF, Constable IJ, Chu Y, Wiffen S. A quantitative study of the lateral spread of Müller cell responses to retinal lesions in the rabbit. *J Comp Neurol*. 1993;334:545-558.
- Behar-Cohen FF, Thillaye-Goldenberg B, de Bizemont T, et al. EIU in the rat promotes the potential of syngeneic retinal cells injected into the vitreous cavity to induce PVR. *Invest Ophthalmol Vis Sci*. 2000;41:3915-3924.
- Sherry DM, Townes-Anderson E. Rapid glutamatergic alterations in the neural retina induced by retinal detachment. *Invest Ophthalmol Vis Sci*. 2000;41:2779-2790.
- Szabo ME, Droy-Lefaix MT, Doly M, Carre C, Braquet P. Ischemia and reperfusion-induced histological changes in the rat retina: demonstration of a free radical-mediated mechanism. *Invest Ophthalmol Vis Sci*. 1991;32:1471-1478.
- Grimm C, Wenzel A, Hafezi F, Reme CE. Gene expression in the mouse retina: the effect of damaging light. *Mol Vis*. 2000;6:252-260.
- Yoshimura N, Kikuchi T, Kuroiwa S, Gaun S. Differential temporal and spatial expression of immediate early genes in retinal neurons after ischemia-reperfusion injury. *Invest Ophthalmol Vis Sci*. 2003;44:2211-2220.
- Bringmann A, Reichenbach A. Role of Müller cells in retinal degenerations. *Front Biosci*. 2001;6:E72-E92.
- Grierson I, Hiscott P, Hogg P, Robey H, Mazure A, Larkin G. Development, repair and regeneration of the retinal pigment epithelium. *Eye*. 1994;8:255-262.
- Sahel JA, Albert DM, Lessell S, Adler H, McGee TL, Konrad-Rastegar J. Mitogenic effects of excitatory amino acids in the adult rat retina. *J Exp Eye Res*. 1991;53:657-664.
- Bignami A, Dahl D. The radial glia of Müller in the rat retina and their response to injury: an immunofluorescence study with antibodies to the glial fibrillary acidic (GFA) protein. *Exp Eye Res*. 1979;28:63-69.
- Clarke K, Geisert EE Jr. The target of the antiproliferative antibody (TAPA) in the normal and injured rat retina. *Mol Vision*. 1998;4:3.
- Song BK, Geisert GR, Vazquez-Chona F, Geisert EE Jr. Temporal regulation of CD81 following retinal injury in the rat. *Neurosci Lett*. 2003;338:29-32.

17. Geller SF, Lewis GP, Fisher SK. FGFR1, signaling, and AP-1 expression after retinal detachment: reactive Müller and RPE cells. *Invest Ophthalmol Vis Sci.* 2001;42:1363-1369.
18. Dijkstra S, Geisert EE Jr, Gispén WH, Bar PR, Joosten EA. Up-regulation of CD81 (target of the antiproliferative antibody; TAPA) by reactive microglia and astrocytes after spinal cord injury in the rat. *J Comp Neurol.* 2000;428:266-277.
19. Geisert EE Jr, Yang L, Irwin MH. Astrocyte growth, reactivity, and the target of the antiproliferative antibody, TAPA. *J Neurosci.* 1996;16:5478-5487.
20. Sullivan CD, Geisert EE Jr. Expression of rat target of the antiproliferative antibody (TAPA) in the developing brain. *J Comp Neurol.* 1998;396:366-380.
21. MacLaren RE. Development and role of retinal glia in regeneration of ganglion cells following injury. *Br J Ophthalmol.* 1996;80:458-464.
22. Miller NM, Oberdorfer M. Neuronal and neuroglial responses following retinal lesions in the neonatal rats. *J Comp Neurol.* 1981;202:493-504.
23. Rogojina AT, Orr WE, Song BK, Geisert EE Jr. Comparing the use Affymetrix to spotted oligonucleotide microarrays using two retinal pigment epithelium cell lines. *Mol Vis.* 2003;9:482-496.
24. Irizarry RA, Bolstad BM, Collin F, Cope LM, Hobbs B, Speed TP. Summaries of Affymetrix GeneChip probe level data. *Nucleic Acids Res.* 2003;31:e15.
25. Reiner A, Yekutieli D, Benjamini Y. Identifying differentially expressed genes using false discovery rate controlling procedures. *Bioinformatics.* 2003;19:368-375.
26. Peterson LE. CLUSFAVOR 5.0 hierarchical cluster and principal component analysis of microarray-based transcriptional profiles. *Genome Biol.* 2002;3:SOFTWARE0002.
27. Cho EY, Choi HL, Chan FL. Expression pattern of glycoconjugates in rat retina as analyzed by lectin histochemistry. *Histochemical J.* 2002;34:589-600.
28. Liou GI, Pakalnis VA, Matragoon S, et al. HGF regulation of RPE proliferation in an IL-1B/retinal hole-induced rabbit model of PVR. *Mol Vis.* 2002;8:494-501.
29. Matzilevich DA, Rall JM, Moore AN, Grill RJ, Dash PK. High-density microarray analysis of hippocampal gene expression following experimental brain injury. *J Neurosci Res.* 2002;67:646-663.
30. Di Giovanni S, Knobloch SM, Brandoli C, Aden SA, Hoffman EP, Faden AI. Gene profiling in spinal cord injury shows role of cell cycle in neuronal death. *Ann Neurol.* 2003;53:454-468.
31. Ridet JL, Malhotra SK, Privat A, Gage FH. Reactive astrocytes: cellular and molecular cues to biological function. *Trends Neurosci.* 1997;20:570-577.
32. Strunnikova N, Baffi J, Gonzalez A, Silk W, Cousins SW, Csaky KG. Regulated heat shock protein 27 expression in human retinal pigment epithelium. *Invest Ophthalmol Vis Sci.* 2001;42:2130-2138.
33. Wong P, Ulyanova T, Organisciak DT, et al. Expression of multiple forms of clusterin during light-induced retinal degeneration. *Curr Eye Res.* 2001;23:157-165.
34. Wu T, Chen Y, Chiang SK, Tso MO. NF-kappaB activation in light-induced retinal degeneration in a mouse model. *Invest Ophthalmol Vis Sci.* 2002;43:2834-2840.
35. Heyer LJ, Kruglyak S, Yooshep S. Exploring expression data: identification and analysis of coexpressed genes. *Genome Res.* 1999;9:1106-1115.
36. Spellman PT, Sherlock G, Zhang MQ, et al. Comprehensive identification of cell cycle-regulated genes of the yeast *Saccharomyces cerevisiae* by microarray hybridization. *Mol Biol Cell.* 1998;9:3273-3297.
37. Chen L, Dentichev T, Wong R, et al. Increased expression of ceruloplasmin in the retina following photic injury. *Mol Vis.* 2003;30:9:151-158.
38. Wang Y, Smith SB, Ogilvie JM, McCool DJ, Sarthy V. Ciliary neurotrophic factor induces glial fibrillary acidic protein in retinal Müller cells through the JAK/STAT signal transduction pathway. *Curr Eye Res.* 2002;24:305-312.
39. Anderson DH, Ozaki S, Nealon M, et al. Local cellular sources of apolipoprotein E in the human retina and retinal pigmented epithelium: implications for the process of drusen formation. *Am J Ophthalmol.* 2001;131:767-781.
40. Gilbert RE, Cox AJ, Kelly DJ, et al. Localization of secreted protein acidic and rich in cysteine (SPARC) expression in the rat eye. *Connect Tissue Res.* 1999;40:295-303.
41. Tanaka S, Suzuki K, Watanabe M, Matsuda A, Tone S, Koike T. Upregulation of a new microglial gene, *mrf-1*, in response to programmed neuronal cell death and degeneration. *J Neurosci.* 1998;18:6358-6369.
42. Trencia A, Perfetti A, Cassese A, et al. Protein kinase B/Akt binds and phosphorylates PED/PEA-15, stabilizing its antiapoptotic action. *Mol Cell Biol.* 2003;23:4511-4521.
43. Atanasoski S, Scherer SS, Nave KA, Suter U. Proliferation of Schwann cells and regulation of cyclin D1 expression in an animal model of Charcot-Marie-Tooth disease type 1A. *J Neurosci Res.* 2002;67:443-449.
44. Acarin L, Gonzalez B, Castellano B. Glial activation in the immature rat brain: implication of inflammatory transcription factors and cytokine expression. *Prog Brain Res.* 2001;132:375-389.
45. Horvath CM. STAT proteins and transcriptional responses to extracellular signals. *Trends Biochem Sci.* 2000;25:496-502.
46. Horwitz J. Alpha-crystallin. *Exp Eye Res.* 2003;76:145-153.
47. Piatigorsky J. Multifunctional lens crystallins and corneal enzymes: more than meets the eye. *Ann N Y Acad Sci.* 1998;842:7-15.
48. Alge CS, Priglinger SG, Neubauer AS, et al. Retinal pigment epithelium is protected against apoptosis by alphaB-crystallin. *Invest Ophthalmol Vis Sci.* 2002;43:3575-3582.
49. Sakaguchi H, Miyagi M, Darrow RM, et al. Intense light exposure changes the crystallin content in retina. *Exp Eye Res.* 2003;76:131-133.
50. Xi J, Farjo R, Yoshida S, Kern TS, Swaroop A, Andley UP. A comprehensive analysis of the expression of crystallins in mouse retina. *Mol Vis.* 2003;9:410-419.
51. Boucheix C, Rubinstein E. Tetraspanins. *Cell Mol Life Sci.* 2001;58:1189-1205.
52. Hemler ME. Specific tetraspanin functions. *J Cell Bio.* 2001;55:1103-1107.
53. Szollosi J, Horejsi V, Bene L, Angelisova P, Damjanovich S. Supramolecular complexes of MHC class I, MHC class II, CD20, and tetraspan molecules (CD53, CD81, and CD82) at the surface of a B cell line JY. *J Immunol.* 1996;157:2939-2946.